Nonparametric time-variant frequency response function estimates using arbitrary excitations

Pintelon, Rik; Louarroudi, Ebrahim; Lataire, John

Published in:
Automatica

DOI:
10.1016/j.automatica.2014.10.088

Publication date:
2015

Nonparametric Time-Variant Frequency Response Function Estimates Using Arbitrary Excitations

R. Pintelon, E. Louarroudi, and J. Lataire

Vrije Universiteit Brussel, dept. ELEC, Pleinlaan 2, 1050 Brussel, Belgium

Tel. (+32-2) 629.29.44, Fax. (+32-2) 629.28.50, E-mail: Rik.Pintelon@vub.ac.be

Abstract

The time-variant frequency response function (TV-FRF) uniquely characterizes the dynamic behaviour of a linear time-variant (LTV) system. This paper proposes a method for estimating nonparametrically the dynamic part of the TV-FRF from known input, noisy output observations. The arbitrary time-variation of the TV-FRF is modelled by Legendre polynomials. In opposition to existing solutions, the proposed method is applicable to arbitrary inputs.

Keywords: time-variant frequency response function, nonparametric estimates, arbitrary excitations, time-variant systems, Legendre polynomials

1. Introduction

Time-variant dynamics are present in all kinds of engineering applications, and they can be classified according to the nature of the time-variation. Either the time-variation is due to a physical phenomenon or a (scheduling) parameter that varies smoothly as a function of time (class A), or it is induced by the switching between a finite number of linear time-invariant systems (class B). Examples of class A dynamics are, thermal drift in power electronics (Chen and Yuang, 2011); fatigue, aging and mortification in biomedical measurements (Aerts and Dirckx, 2010); pit corrosion of metals (Van Ingelgem *et al.*, 2008); control of crane dynamics (Abdel-Rahman *et al.*, 2003); airplane dynamics during take off and landing (Dimitriadis and Cooper, 2001); and impedance measurements for determining the state-of-charge of batteries (Rodrigues *et al.*, 2000; Pop *et al.*, 2005). Examples of class B dynamics are, regime switching in power electronics (Aguilera *et al.*, 2014), econometrics (Hamilton, 1990), and control applications (Yin *et al.*, 2009); and more general, hybrid systems (see Paoletti *et al.*, 2007 and the references therein).

In this paper we consider class A dynamics only. The time-variant frequency response function (TV-FRF) introduced in Zadeh (1950a,b) provides deep insight into the time-variant behaviour of class A dynamics. Hence, there is a need for methods that estimate the TV-FRF from input-output data. According to the parametrisation used, one can distinguish four model classes for describing the class A dynamics:

1. Parametric in both the dynamics and the time-variation: a lot of estimation algorithms are available, see Niedzwiecki (2000); Poulimenos and Fassois (2006); Tóth et al. (2012) and the references therein. The time- or parameter-variant system is modelled using a differential, difference, or state space equation where the (matrix) coefficients are affine functions of time- or parameter-dependent basis functions, for example, wavelets in Li and Billings (2011), polynomials in Lataire and Pintelon (2011), sines and cosines in Allen (2008) and Louarroudi et al. (2013), or integrated white noise in Kitagawa and Gersch (1985).
2. Parametric in the dynamics and nonparametric in the (slow) time-variation: see Georgiev (1989); Liu (1997); and Niedzwiecki and Kaczmarek (2005).
3. Nonparametric in the dynamics and parametric in the (slow) time-variation: periodic time-variation in Sams and Marmarelis (1988) and Louarroudi et al. (2012) parametrised by sines and cosines; and arbitrary time-variation in Lataire et al. (2012) parametrised by polynomials.
4. Nonparametric in both the dynamics and the (very) slow time-variation: the TV-FRF is estimated using the short-time Fourier transform (Allen and Rabiner, 1977). The basic assumption made is that the system is time-invariant within the short sliding time window: see, for example, Spiridonakos and Fassois (2009) for noise power spectra and Sanchez et al. (2013) for FRFs.

Model classes 1 and 2 require a parametric model for describing the system dynamics, which is not the case for model classes 3 and 4. The latter are natural extensions of the nonparametric FRF representation of linear time-invariant systems. The three disadvantages of parametrising the system dynamics w.r.t. to a nonparametric representation are the following: (i) the type of dynamic model must be chosen: differential equation (s-domain), difference equation (z-domain), fractional differential equation (e.g., $\sqrt{s}$-domain), or partial differential equation; (ii) the dynamic model order must be chosen (orders time-domain derivatives or time-domain shifts of the input and output signals); and (iii) estimating the model parameters mostly involves a nonlinear minimisation. The latter requires the generation of initial estimates and includes possible problems with local minima. The main advantages of parametric models are the compact description and the smaller estimation uncertainty. Nonparametric estimation tech-

niques are very helpful to get an idea of the complexity of the parametric modelling step and to validate the estimated parametric system model.
Compared with the algorithms for model class 3, the methods developed for model class 4 have the disadvantage that they require a trade-off between accurate tracking of the time-variation (the sliding time window should be as small as possible) and sufficiently large frequency resolution of the estimated dynamics (the sliding time window should be as large as possible). In addition, at the cost of a more complicated estimation algorithm, the methods for model class 3 result in TV-FRF estimates with a much larger frequency resolution.

This paper considers the third model class with nonparametric dynamics and arbitrary time-variation parametrised by Legendre polynomials. The approach presented in Lataire et al. (2012) – called the direct method in the sequel of this paper – has the disadvantages that a lot of signal periods are needed and that it is not applicable to random excitations. In this paper an indirect method is proposed that is applicable to arbitrary excitations and a few (less than one) period(s) of periodic inputs.

The paper is organised as follows. First, the class of linear time-variant systems considered and the stochastic framework are defined (Sections 2 and 3). Next, an indirect method for estimating nonparametrically the TV-FRF of this class of systems is developed and analysed in detail (Section 4). Further, the proposed indirect method is compared with the direct approach (Section 5). Finally, the whole procedure is illustrated via measurements on a time-variant electronic circuit (Section 6).

2. The Time-Variant Frequency Response Function

First, we recall the definition and the properties of the time-variant frequency response function (TV-FRF). Next, a nonparametric-in-the-dynamics and parametric-in-the-time-variation representation for a class of (slowly) time-varying systems is given.

2.1. Definition and Properties of the TV-FRF

The dynamic behaviour of a linear time-variant (LTV) system is uniquely characterised by its response $g(t, \tau)$ to a Dirac impulse applied at time instant $t = \tau$ (Zadeh, 1950a,b). Taking the Fourier transform of the shifted time-variant impulse response $g(t, t - \tau)$ defines the TV-FRF, called the system function in Zadeh (1950a,b),

$$G(j\omega, t) = \int_{-\infty}^{+\infty} g(t, t-\tau)\, e^{-j\omega\tau} d\tau. \qquad (1)$$

For causal systems ($g(t, \tau) = 0$ for $t < \tau$) the lower integration boundary in (1) is replaced by zero. The time-variant FRF (1) has the following properties:

1. The steady state response to $\sin(\omega_0 t)$ equals

$$|G(j\omega_0, t)| \sin(\omega_0 t + \angle G(j\omega_0, t)) \qquad (2)$$

which is an amplitude and phase modulated sine wave. Note that the Fourier spectrum of (2) is non-zero in the close neighbourhood of ω_0, resulting in a skirt-like spectrum around ω_0 (see Lataire *et al.*, 2012).

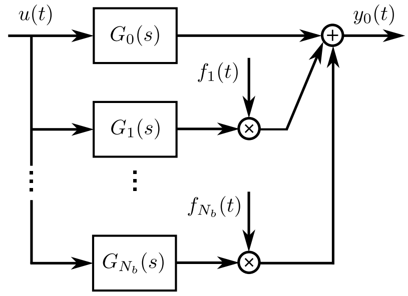

Figure 1: Block diagram of the slowly time-varying system (6) – direct model.

2. Assuming zero initial conditions, the transient response $y_0(t)$ to an input $u(t)$ is found as

$$y_0(t) = L^{-1}\{G(s, t)\, U(s)\} \qquad (3)$$

with $U(s)$ the Laplace transform of $u(t)$, and $L^{-1}\{\}$ the inverse Laplace transform.

Note that properties (2) and (3) are natural extensions of the linear time-invariant (LTI) case.

2.2. Nonparametric Representation of the TV-FRF

The nonparametric representation of the dynamics of the TV-FRF is obtained in two steps.

First, the TV-FRF (1) is expanded in series w.r.t. time

$$G(j\omega, t) = \sum_{r=0}^{\infty} G_r(j\omega)\, f_r(t) \quad t \in [0, T] \qquad (4)$$

with $f_r(t)$, $r = 0, 1, \ldots$, a complete set of basis functions, and T the experiment time. $G_r(j\omega)$, $r = 0, 1, \ldots$, are the complex coefficients of the series expansion which can be interpreted as FRFs of LTI systems. Note that the basis functions can always be chosen such that the constraints

$$f_0(t) = 1 \text{ and } \frac{1}{T}\int_0^T f_r(t)\, dt = 0 \text{ for } r > 0 \qquad (5)$$

are satisfied.

In a second step, the infinite sum (4) is approximated by a finite sum

$$G(j\omega, t) = \sum_{r=0}^{N_b} G_r(j\omega)\, f_r(t) \quad t \in [0, T] \qquad (6)$$

Representation (6) is parametric in the time-variation (the basis functions $f_r(t)$ are known), and nonparametric in the unknown FRFs $G_r(j\omega)$, $r = 0, 1, \ldots, N_b$. Note that in practise N_b is unknown and, hence, should also be estimated from the data.

Eq. (6) motivates the following assumption:

Assumption 1. *(Slow time-variation) The TV-FRF* (1) *of the linear time-variant system can be written as* (6)*, where $f_r(t)$, $r = 0, 1, \ldots, N_b$, are polynomials of order r satisfying* (5).

The term "slow time-variation" in Assumption 1 is justified as follows. For the Legendre polynomials used in the indirect method (see Section 3), the spectral content of $f_r(t)$ is concentrated around DC. However, this does not

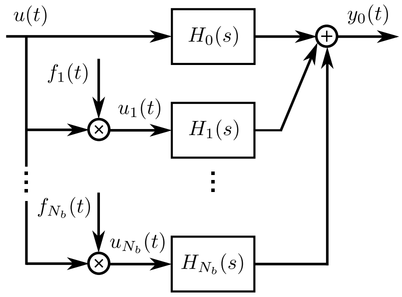

Figure 2: Block diagram of a slowly time-varying system (6) with polynomial basis functions $f_r(t)$ – indirect model. This block diagram is a multiple-input $u(t)$, $u_1(t)$, ..., $u_{N_b}(t)$, single-output $y_0(t)$ LTI equivalent of the single-input $u(t)$, single-output $y_0(t)$ LTV system shown in Fig. 1.

exclude that the time-variation can be strong (large), which is the case if at least one of the amplitudes of $G_r(j\omega)$, $r \geqslant 1$, is not much smaller than that of $G_0(j\omega)$.

3. Stochastic Framework

The indirect method for estimating the TV-FRF (6) is developed within the following stochastic setting.

Assumption 2. *(Generalised output error framework) The input $u(t)$ of the slowly time-variant system* (6) *is known exactly and the output $y_0(t)$ is disturbed by stationary noise $n_y(t)$ ($y(t) = y_0(t) + n_y(t)$), where $n_y(t)$ is independently distributed of $u(t)$.*

If $n_y(t)$ is solely due to measurement noise, then the stationarity assumption is exact without any approximation. However, if $n_y(t)$ is dominated by the process noise, then the stationarity assumption is an approximation because the process noise is affected by the time-variant system dynamics. Nevertheless, weakly time-variant disturbing output noise can be approximated very well by its best (in least squares sense) linear time-invariant approximation (Pintelon *et al.*, 2012), which justifies Assumption 2. Simultaneous nonparametric estimation of the system and disturbing noise dynamics is a challenging unsolved problem that is out of the scope of this paper.

4. The Indirect Method for Estimating the Time-Variant Frequency Response Function

Under Assumption 1, a direct method for estimating nonparametrically the FRFs $G_r(j\omega)$ in (6) from several periods of the response to a periodic excitation, has been developed in Lataire et al. (2012). It requires a large number of signal periods and cannot handle arbitrary excitations. In this section a new approach – called the indirect method – is presented that does not suffer from these drawbacks. It is based on a multiple-input, single-output LTI equivalent model – called the indirect model – of the single-input, single-output LTV system.

4.1. The Indirect Model

In Theorem 2 of Pintelon et al. (2012) it has been shown that for any polynomial basis $f_r(t)$, $r = 0, 1, \ldots, N_b$, there exist transfer functions $H_r(s)$, $r = 0, 1, \ldots, N_b$, such that the response of the time-variant system in Fig. 1 with TV-FRF (6) can be written as

$$y_0(t) = \sum_{r=0}^{N_b} L^{-1}\{G_r(s)U(s)\} f_r(t) \tag{7}$$

$$= L^{-1}\left\{\sum_{r=0}^{N_b} H_r(s) L\{u(t) f_r(t)\}\right\} \tag{8}$$

Eq. (8) is called the indirect model of the slowly time-varying system (6), and the corresponding block diagram is shown in Fig. 2. The following theorem establishes explicitly the relationship between $G_r(s)$ and $H_r(s)$, $r = 0, 1, \ldots, N_b$, for Legendre polynomials as basis functions (in Pintelon *et al.*, 2012 only the relationship between $G_0(s)$, the best linear time-invariant approximation of (6), and $H_r(s)$, $r = 0, 1, \ldots, N_b$, has been proven). No assumption about the initial conditions is made.

Theorem 3. *Let $p_r(2t/T - 1)$, $t \in [0, T]$, be Legendre polynomials of order r (Abramowitz and Stegun, 1970). Choosing $f_r(t) = p_r(2t/T - 1)$ as basis functions, the relationship between the $G_r(s)$* (7) *and the $H_r(s)$* (8) *transfer functions is given by*

$$G_r(s) = H_r(s) + \frac{2}{T}(2r+1) \sum_{i=0}^{\left\lfloor \frac{N_b-r-1}{2} \right\rfloor} H^{(1)}_{2i+1+r}(s) + \frac{4}{T^2} \sum_{i=1}^{\left\lfloor \frac{N_b-r}{2} \right\rfloor} \beta_{2i,r} H^{(2)}_{2i+r}(s) + O\left(T^{-3}\right) \tag{9}$$

with $\lfloor x \rfloor$ the largest integer smaller than or equal to x, $H_r^{(m)}(s)$ the m-th order derivative of $H_r(s)$ w.r.t. s, $\beta_{2i,r}$ the following coefficients

$$\begin{aligned} \beta_{2i,r} &= \gamma_r + \delta_r (i-1) + \mu_r (i-1)^2 \\ \gamma_r &= 1.5 + 4r + 2r^2 \\ \delta_r &= 2.5 + 6r + 2r^2 \\ \mu_r &= 1 + 2r \end{aligned} \tag{10}$$

and where $O(T^{-n})$ with $n > 0$ means that $\lim_{T\to\infty} T^n O(T^{-n}) < \infty$. The $O\left(T^{-3}\right)$ bias term in (9) *depends on the higher order derivatives $H_q^{(m)}(s)$, with $N_b \geqslant q \geqslant r + 3$, and where m ranges from $3 + (q + 1 + r) \bmod 2$ to $q - r$ in steps of 2 (*mod *stands for modulo).*

Proof. See the Appendix. □

There is an important conceptual difference between Eq. (7), visualized in Fig. 1, and Eq. (8), visualized in Fig. 2. Indeed, Eq. (7) represents a single-input $u(t)$, single-output $y_0(t)$ LTV system, while Eq. (8) can be interpreted as a multiple-input $u(t)$, $u_1(t)$, ..., $u_{N_b}(t)$, single-output $y_0(t)$ (MISO) LTI system (the basis functions $f_r(t)$ are known). The transfer functions $H_0(s)$, $H_1(s)$, ..., $H_{N_b}(s)$ in the MISO LTI representation (8) are identifiable for persistently exciting inputs $u(t)$ because $u(t)$, $u_1(t)$, ..., $u_{N_b}(t)$ are linearly independent.

Lemma 4. *The N_b+1 inputs $u(t)$, $u_1(t)$, …, $u_{N_b}(t)$ are linearly independent for non-zero inputs $u(t)$.*

Proof. Since $f_r(t)$, $r = 0, 1, \ldots, N_b$, are linearly independent (they form a basis), and since $u(t) \neq 0$, the linear combination $\sum_{r=0}^{N_b} \alpha_r u_r(t) = u(t) \sum_{r=0}^{N_b} \alpha_r f_r(t)$ can only be zero for all $t \in [0, T]$ if and only if $\alpha_r = 0$, $r = 0, 1, \ldots, N_b$. □

The important consequence of these observations is that standard (non)parametric LTI techniques can be used for estimating the dynamics $H_r(j\omega)$, $r = 0, 1, \ldots, N_b$.

4.2. The Indirect Method

4.2.1. Identifiability

A persistence of excitation condition on $u(t)$ is sufficient to guarantee the identifiability of the parametric transfer functions $H_r(s)$, $r = 0, 1, \ldots, N_b$ (see Lemma 4). The nonparametric estimation of the FRFs $H_r(j\omega)$, $r = 0, 1, \ldots, N_b$, however, imposes additional conditions on the excitation $u(t)$: in the frequency band of interest the input discrete Fourier transform (DFT) spectrum $U(k)$ of $u(t)$

$$U(k) = \mathrm{DFT}(u(t)) = \frac{1}{\sqrt{N}} \sum_{n=0}^{N-1} u(nT_s)\, e^{-j2\pi kn/N} \tag{11}$$

with T_s the sampling period ($NT_s = T$), should vary "wildly" enough over the frequencies to ensure identifiability. For example, the spectral analysis method requires a "roughness" condition on the input DFT spectrum: $|\mathrm{diff}^{(m)}(U(k))| = O(N^0)$ in probability, with $\mathrm{diff}^{(m)}(U(k)) = \mathrm{diff}(\mathrm{diff}^{(m-1)}(U(k)))$ and $\mathrm{diff}(U(k)) = U(k+1) - U(k)$, see Schoukens et al. (2009).

In this paper the local polynomial method (LPM) is used because it delivers nonparametric FRF estimates at the full frequency resolution $1/T$ of the experiment, while suppressing better the leakage (transient) errors than the spectral analysis approach (Pintelon and Schoukens, 2012; Pintelon *et al.*, 2010). For the LPM, the identifiability condition on the input DFT spectrum $U(k)$ is formulated in the following assumption.

Assumption 5. *(Identifiability condition) The $(R+1)(N_b+2) \times (2n+1)$ regression matrix $K_n(k)$*

$$K_n(k) = \left[\ K(k-n) \cdots K(k) \cdots K(k+n)\ \right] \tag{12}$$
$$K(k+r) = \begin{bmatrix} \tilde{K}(r) \otimes U_{\mathrm{all}}(k) \\ \tilde{K}(r) \end{bmatrix}$$
$$\tilde{K}(r) = \left[1\ r\ \cdots\ r^R\right]^T$$
$$U_{\mathrm{all}}(k) = \left[U(k)\, U_1(k) \cdots U_{N_b}(k)\right]^T$$

with R the order of the local polynomial approximation of the FRFs and the leakage (transient) error in the local frequency band $[k-n, k+n]$, $U_r(k) = \mathrm{DFT}(f_r(t)u(t))$ (see Eq. (11)), and $\otimes$ the Kronecker matrix product, is of full row rank at all frequencies k of interest.

It can be verified that Assumption 5 is fulfilled for filtered white noise and random phase multisine excitations.

4.2.2. Algorithm

The algorithm is a two step procedure that is valid for any initial condition. First, under Assumptions 1, 2, and 5 the FRFs in the indirect model (8) are estimated and, next, using Theorem 3, the indirect model (8) is transformed into the direct model (7).

Step 1

Taking the DFT (11) of (8) gives

$$Y_0(k) = \sum_{r=0}^{N_b} H_r(j\omega_k)\, U_r(k) + T_H(j\omega_k) \tag{13}$$

with $U_r(k)$ defined in Assumption 5, $Y_0(k) = \mathrm{DFT}(y_0(t))$, and where $T_H(j\omega_k) = O(T^{-1/2})$ is a rational function of the frequency modelling the sum of the leakage (transient) error and the residual alias error. The leakage error is due to the difference between the initial ($t = 0$) and final ($t = T$) conditions of the experiment, while the residual alias error originates from the time-limited observation of a band-limited signal (see Pintelon and Schoukens, 1997; and Theorem 5 of Pintelon *et al.*, 2012). Starting from N known input, N noisy output samples $u(nT_s)$, $y(nT_s)$, $n = 0, 1, \ldots, N-1$, the FRFs $H_r(j\omega_k)$, $r = 0, 1, \ldots, N_b$, the transient term $T_H(j\omega_k)$ and their noise covariances are estimated nonparametrically using the local polynomial method (Pintelon *et al.*, 2010; Pintelon and Schoukens, 2012).

The local bandwidth $2n+1$ and the order R of the local polynomial approximation of $H_r(j\omega_k)$, $r = 0, 1, \ldots, N_b$, and $T_H(j\omega_k)$ are chosen such that 1) the bias error of the FRF estimates is below the variance error, and 2) the noise covariance estimate has the required quality. The latter is quantified by the degrees of freedom

$$\mathrm{dof} = 2n + 1 - (R+1)(N_b+2) \tag{14}$$

which is the difference between the number of frequencies in the local frequency band $[k-n, k+n]$ and the number of estimated local parameters. Requirement 1) is satisfied when the mean square error of the residuals of the local polynomial approximation does not decrease any-more for increasing values of R.

In practise the number of time-variant branches N_b in (13) is unknown and should also be estimated from the data. This is done as follows. We start with $N_b = 0$ and increase its value until $|H_p(j\omega_k)| \sim \mathrm{std}(H_p(j\omega_k))$ over the whole frequency band for $p > N_b$.

Step 2

Using (9), a nonparametric estimate of the FRFs $G_r(j\omega_k)$, $r = 0, 1, \ldots, N_b$, in the direct model (7) is obtained as

$$\hat{G}_r(j\omega_k) = \hat{H}_r(j\omega_k) + \frac{2}{T}(2r+1) \sum_{i=0}^{\left\lfloor \frac{N_b - r - 1}{2} \right\rfloor} \hat{H}^{(1)}_{2i+1+r}(j\omega_k) \tag{15}$$

where the first-order derivatives are replaced by first-order central differences

$$\hat{H}^{(1)}_m(j\omega_k) = \frac{\hat{H}_m(j\omega_{k+1}) - \hat{H}_m(j\omega_{k-1})}{j\omega_{k+1} - j\omega_{k-1}} \tag{16}$$

The estimate (15) can be improved as

$$\hat{\hat{G}}_r(j\omega_k) = \hat{G}_r(j\omega_k) + \frac{4}{T^2}\sum_{i=1}^{\left\lfloor\frac{N_b-r}{2}\right\rfloor}\beta_{2i,r}\hat{H}^{(2)}_{2i+r}(j\omega_k) \quad (17)$$

where the second-order derivatives are replaced by second-order central differences

$$\hat{H}^{(2)}_m(j\omega_k) = \frac{\hat{H}_m(j\omega_{k+2}) - 2\hat{H}_m(j\omega_k) + \hat{H}_m(j\omega_{k-2})}{(j\omega_{k+1} - j\omega_{k-1})^2} \quad (18)$$

Finally, replacing $G_r(j\omega_k)$ in (6) by (15) or (17) gives the nonparametric TV-FRF estimate $\hat{G}(j\omega_k, t)$ and $\hat{\hat{G}}(j\omega_k, t)$ respectively. Since the correlation length over the frequency of the LPM estimates $\hat{H}_r(j\omega_k)$ is $\pm 2n$ (Pintelon *et al.*, 2010); the correlation length of the estimates $\hat{G}(j\omega_k, t)$ and $\hat{\hat{G}}(j\omega_k, t)$ is, respectively, $\pm(2n+1)$ and $\pm(2n+2)$.

4.2.3. Stochastic Properties

Bias Error

Since the central differences (16) and (18) equal the true derivatives within an $O(T^{-2})$ bias error (Ralston and Rabinowitz, 1984); and since the bias error of the LPM estimate is an $O(T^{-(R+1)})$, with R the order of the local polynomial approximation (Pintelon *et al.*, 2010; Pintelon and Schoukens, 2012); it follows from (9), (15) and (17) that the biases $b_{\hat{G}_r}(j\omega_k) = \mathbb{E}\{\hat{G}_r(j\omega_k)\} - G_r(j\omega_k)$ and $b_{\hat{\hat{G}}_r}(j\omega_k) = \mathbb{E}\{\hat{\hat{G}}_r(j\omega_k)\} - G_r(j\omega_k)$ are given by

$$b_{\hat{G}_r}(j\omega_k) = \frac{4}{T^2}\sum_{i=1}^{\left\lfloor\frac{N_b-r}{2}\right\rfloor}\beta_{2i,r}H^{(2)}_{2i+r}(j\omega_k) + O\left(T^{-3}\right) \quad (19)$$

$$b_{\hat{\hat{G}}_r}(j\omega_k) = O\left(T^{-3}\right) \quad (20)$$

respectively. The first term in the right hand side of (19) is an $O(T^{-2})$ that can be estimated using (18).

Finally, replacing $G_r(j\omega_k)$ in (6) by $b_{\hat{G}_r}(j\omega_k)$ (19) and $b_{\hat{\hat{G}}_r}(j\omega_k)$ (20) gives the bias of $\hat{G}(j\omega_k, t)$ and $\hat{\hat{G}}(j\omega_k, t)$ respectively.

Variance Error

The variance of the estimated TV-FRF $\hat{G}(j\omega_k, t)$ (6) depends on the covariances of $\hat{G}_r(j\omega_k)$, $r = 0, 1, \ldots, N_b$. It follows from (15) that these covariances depend on the covariances $\hat{H}_r(j\omega_k)$, $r = 0, 1, \ldots, N_b$, and the covariances between $\hat{H}_r(j\omega_k)$ and $\hat{H}_m(j\omega_l)$ for $k-l = -2, -1, 1, 2$. The latter are estimated from the residuals of the LPM estimates of the indirect model (follow the same lines of Pintelon *et al.*, 2010). To calculate the variance of $\hat{\hat{G}}_r(j\omega_k)$, also the covariances between $\hat{H}_r(j\omega_k)$ and $\hat{H}_m(j\omega_l)$ for $k-l = -4, -3, 3, 4$ are needed (see Eqs. (17) and (18)).

Note that the variance of the nonparametric TV-FRF estimates decreases with increasing values of the degrees of freedom dof (14), at the cost of an increased correlation length over the frequency (see Section 4.2.2). In addition, the dof value cannot be chosen too large for a fixed value of R; otherwise the bias will dominate the mean square error of the LPM estimates.

5. Comparison with the Direct Method

5.1. The Direct Method

The direct method starts from the steady state response to a random phase multisine excitation

$$u(t) = \sum_{k=k_1}^{k_2} A_k \sin(2\pi k f_0 t + \phi_k) \quad (21)$$

consisting of the sum of $F = k_2 - k_1 + 1$ harmonically related sinewaves with user defined deterministic amplitudes A_k, and randomly selected phases ϕ_k such that $\mathbb{E}\{e^{j\phi_k}\} = 0$. The DFT spectra (11) of P consecutive periods of the input-output signals satisfy

$$Y_0(k) = G_0(j\omega_k)U(k) + \sum_{p=1}^{N_b}\tilde{Y}_p(k) \quad (22)$$

$$\tilde{Y}_p(k) = \sum_{r=-F, r\neq 0}^{F} G_p(j\omega_{rP})U(rP)\frac{F_p(k-rP)}{\sqrt{N}} \quad (23)$$

where $F_p(k) = \mathrm{DFT}(f_p(t))$, $\omega_{rP} = 2\pi r f_0$, and $f_0 = Pf_s/N$ (proof: take the DFT of the direct model (7) using the fact that $U(k)$ is different from zero for $k = rP$, $r = \pm1, \pm2, \ldots, \pm F$ only and that $U(-k) = \overline{U}(k) = U(N-k)$). Eqs. (22) and (23) show that the response to a random phase multisine excitation consists of the sum of scaled and frequency-shifted copies of the DFT spectra $F_p(k)$ of the time-varying gains $f_p(t)$.

Since $Y_0(k)$ (22) is coupled with $Y_0(k')$ for any k' via (23), estimating the frequency response functions (FRFs) $G_p(j\omega_r)$, $p = 0, 1, \ldots, N_b$ and $r = k_1, k_1+1, \ldots, k_2$, results in a (very) large set $((N/2)\times(N/2))$ of equations. To circumvent this bottleneck, the sum in (22) is approximated in a limited frequency band $k \in [(r-1)P - P/2, (r+1)P + P/2]$ around the excited frequency $k = rP$ as

$$\sum_{p=1}^{N_b}\tilde{Y}_p(k) \approx \sum_{p=1}^{N_b}\sum_{r_1=r-1,}^{r+1} G_p(j\omega_{r_1P})U(r_1P)\frac{F_p(k-r_1P)}{\sqrt{N}} + I(j\omega_k) \quad (24)$$

where $I(j\omega) = \sum_{m=0}^{n_i} i_m (j\omega)^m$ is a polynomial of order n_i modelling the skirts originating from the excited frequencies in (22) that have been neglected in (24). Combining (22)–(24) in the frequency band $k \in [(r-1)P - P/2, (r+1)P + P/2]$ gives a set of $3P+1$ linear equations in $3(N_b+1) + n_i + 1$ unknowns $G_p(j\omega_{r_1})$, $p = 0, 1, \ldots, N_b$ and $r_1 = r-1, r, r+1$, and i_m, $m = 0, 1, \ldots, n_i$. These equations can be solved in least squares sense if

$$3P + 1 > 3(N_b+1) + n_i + 1 \quad (25)$$

is satisfied. The whole procedure is repeated for all excited frequencies k.

5.2. Bias Error

The bias of the direct method (see Section 5.1) is due to the polynomial approximation of the skirts of the out of band excited frequencies in Eq. (24). It depends on the local bandwidth $3P+1$ and the order n_i of the polynomial approximation

$$O\left((3P/N)^{n_i+1}\right) \tag{26}$$

where the number of periods P should be chosen such that (25) is satisfied. Increasing n_i decreases the bias (26).

The bias of the indirect method (see Section 4.2.3) is mainly due to the local polynomial approximation of the FRFs in the indirect model (13), and the bias in the transformation of the indirect to the direct model (9)

$$O\left(N^{-3}\right) + O\left((nP/N)^{R+1}\right) \tag{27}$$

where n is chosen such that dof (14) is strictly positive. Increasing the order R of the local polynomial approximation, or decreasing the number of signal periods P for a fixed measurement time, decreases the bias (27).

5.3. Variance Error

The indirect method imposes a smoothness condition over the frequency on the TV-FRF (6) via a local polynomial approximation of the FRFs in the indirect model (13). Since no smoothness condition over the frequency is imposed on the direct TV-FRF estimate, the variance of the indirect estimate will be smaller than that of the direct estimate for a comparable number of local equations and parameters. The drawback of the smoothing is that it introduces a correlation over the frequency (see Section 4.2.2).

5.4. Identifiability

The identifiability condition (25) of the direct method imposes the number of observed signal periods P to be sufficiently large. This is not the case for the indirect method: it also works for one observed signal period or less ($P \leqslant 1$).

5.5. Choice Basis Functions

For the direct method any basis satisfying (5) can be used, e.g. splines that are localised in time (Eq. (24) remains valid). This is not the case for the indirect method: relationship (10) is valid for Legendre polynomials only.

6. Measurement Example

Although formulas (9) and (10) have extensively been verified on simulations examples satisfying Assumption 1, we prefer to report the results of a measurement example where condition (6) has not been imposed by construction.

6.1. Experimental Set Up

The time-variant electronic circuit is a second order bandpass filter where the time-variation originates from the varying gate voltage $p(t)$ of the JFET transistor (see Fig. 3). It is excited by a random phase multisine $u(t)$ (21) consisting of $F = 33387$ harmonically related sinewaves in the band $[200\,\text{Hz}, 40\,\text{kHz}]$, where $f_0 = f_s/N_0$, $N_0 = 2^{17}$, $f_s = 156.25\,\text{kHz}$, $k_1 = 168$, and $k_2 = 33554$. The amplitudes A_k, $k = k_1, k_1+1, \ldots, k_2$, are constant and chosen such that rms value of $u(t)$ is 93 mV, while the phases ϕ_k, $k = k_1, k_1+1, \ldots, k_2$, are randomly selected according to a

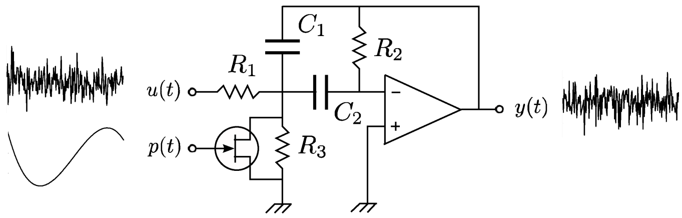

Figure 3: Second order bandpass filter with time-varying resonance frequency and damping ratio. The electronic circuit with input $u(t)$ and output $y(t)$ consists of a high gain operational amplifier (CA741CE), a JFET transistor (BF245B) with gate voltage $p(t)$, three resistors ($R_1 = R_2 = 10\,\text{k}\Omega$ and $R_3 = 470\,\text{k}\Omega$), and two capacitors ($C_1 = C_2 = 10\,\text{nF}$).

uniform $[0, 2\pi)$ distribution. Only $N = 7N_0/8$ data points of the input $u(t)$ and the noisy response $y(t)$ (see Fig. 3) are used for estimating nonparametrically the TV-FRF (6). Over the measurement time $T = NT_s$, with $T_s = 1/f_s$, the gate voltage varies between -1.54 V and -2.14 V (see Fig. 3, and the bottom right plot of Fig. 6).

6.2. Estimation Results

Starting from the N known input and N noisy output samples $u(nT_s)$ and $y(nT_s)$, $n = 0, 1, \ldots, N-1$, the time-variant FRF (6) is estimated for increasing values of N_b following the procedure of Section 4.2.2, with $R = 4$ and dof $= 200$. For $N_b > 9$, the estimated FRFs $\hat{H}_r(j\omega_k)$, $k = 10, 11, \ldots$, are of the same order of magnitude as their standard deviation in the band $[200\,\text{Hz}, 40\,\text{kHz}]$, viz. $|\hat{H}_r(j\omega_k)| \sim \text{std}(\hat{H}_r(j\omega_k))$. Therefore, the number of significant time-variant branches in the indirect model of Fig. 2 equals $N_b = 9$, and the corresponding FRFs are shown in Fig. 4. From this figure it can be seen that the frequency band where the estimated FRF $\hat{H}_r(j\omega_k)$ is significantly above the noise level decreases for increasing values of r.

Using Eqs. (15)–(18), the FRFs $G_r(j\omega_k)$, $r = 1, 2, \ldots, N_b$, in the direct model of Fig. 1 are estimated (see Fig. 5). Compared with the indirect estimates $\hat{H}_r(j\omega_k)$ in Fig. 4, the uncertainty of $\hat{\hat{G}}_r(j\omega_k)$ in Fig. 5 is slightly larger. Combining the $\hat{\hat{G}}_r(j\omega_k)$ estimates with (6) gives the time-variant frequency response function shown in the top row of Fig. 6. As expected, it can be seen from the bottom row of Fig. 6 that the time-dependency of the resonance frequency (the largest amplitude in the time-frequency plot) has the same shape as the gate voltage $p(t)$.

Note that $\hat{\hat{G}}_0(j\omega_k)$, shown in the top left plot of Fig. 5, is an estimate of the best – in least squares sense – linear time-invariant approximation of the time-variant electronic circuit (see Pintelon *et al.*, 2012 for the details). It is also the mean value of the TV-FRF over the interval $[0, T]$ (combine (5) and (6)).

7. Conclusions

This paper has presented an indirect method for estimating nonparametrically the dynamics of the TV-FRF of linear time-variant systems, where the arbitrary time-variation is modelled by Legendre polynomials. The key idea consists in transforming the single-input, single-output

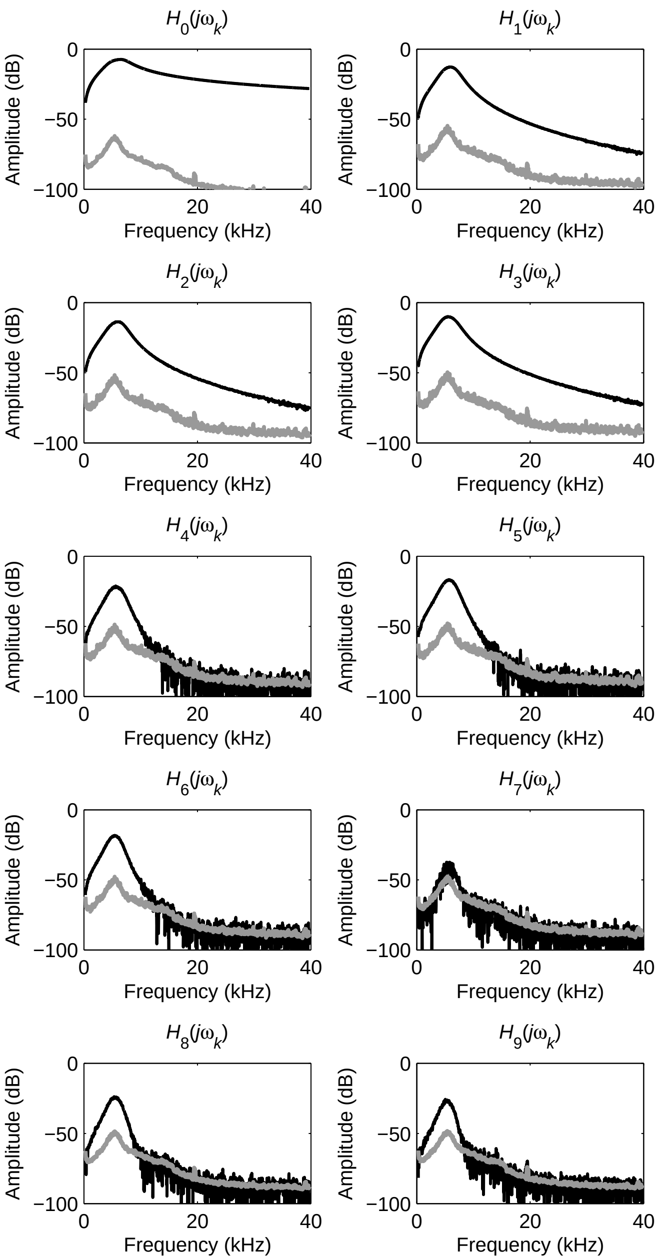

Figure 4: Estimated indirect model (8) of the electronic circuit (see also Fig. 2): FRFs $H_r(j\omega_k)$ (black) and their variance (grey).

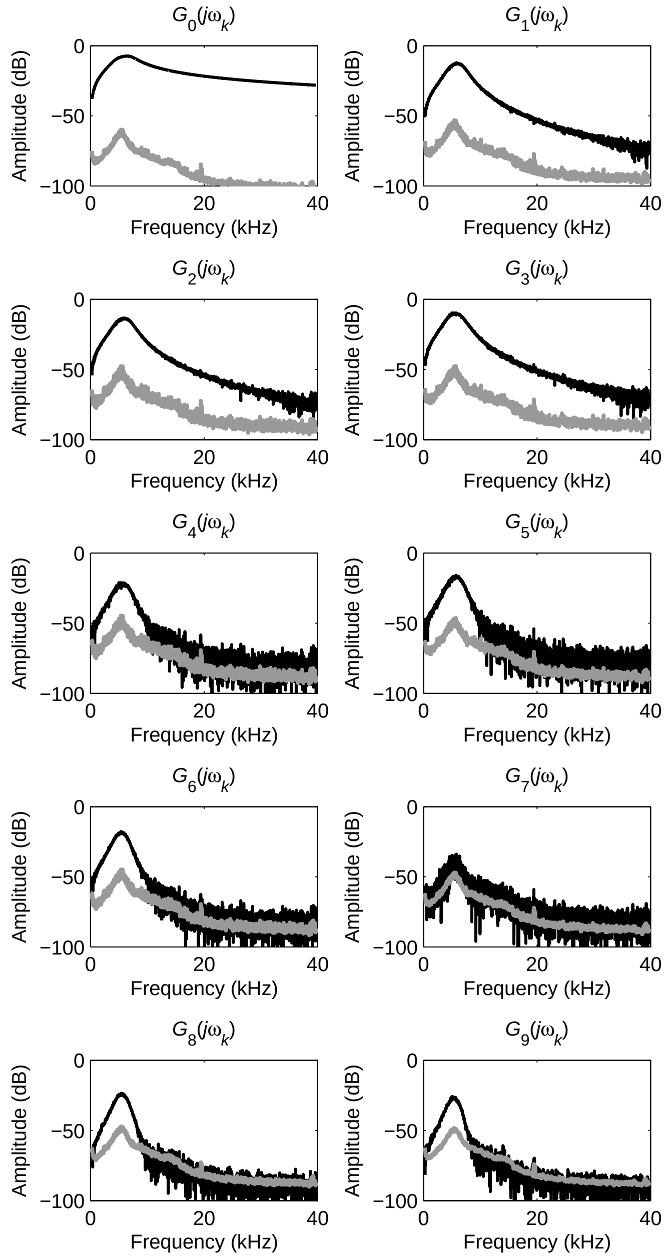

Figure 5: Estimated direct model (7) of the electronic circuit (see also Fig. 1): FRFs $G_r(j\omega_k)$ (black) and their variance (grey).

linear time-variant problem (direct model) into an equivalent multiple-input, single-output linear time-invariant problem (indirect model). Proceeding in this way, standard multiple-input, single output nonparametric methods for LTI systems can be used for estimating the TV-FRF. In opposition to the existing direct method, the proposed solution can handle arbitrary excitations and a very few (less than one) periods of a periodic input.

Acknowledgements

This work is sponsored by the Research Council of the Vrije Universiteit Brussel, the Research Foundation Flanders (FWO-Vlaanderen), the Flemish Government (Methusalem Fund METH1), and the Belgian Federal Government (Interuniversity Attraction Poles programme IAP VII, DYSCO).

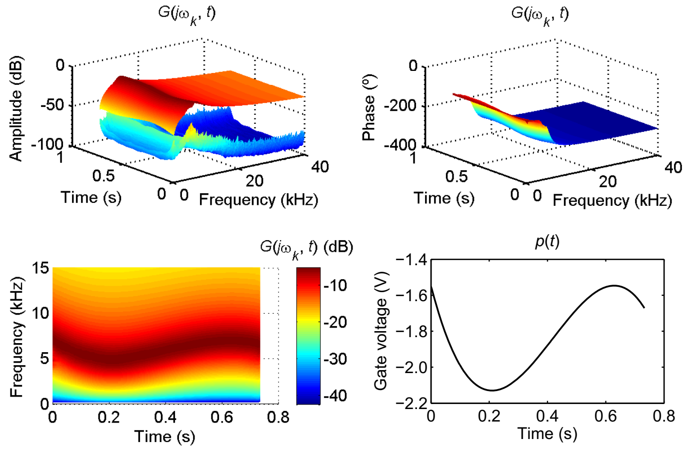

Figure 6: Estimated TV-FRF $G(j\omega_k, t)$ of the electronic circuit. Top left: amplitude (red) and variance (blue) of $G(j\omega_k, t)$; top right: phase of $G(j\omega_k, t)$; bottom left: time-frequency plot of $|G(j\omega_k, t)|$; and bottom right: gate voltage $p(t)$.

Appendix. Proof of Theorem 3

We prove the theorem by induction. First, we show that the theorem is valid for $N_b = 1, 2, \ldots, 11$. Next, via an induction step we show that the theorem is valid for any value of N_b.

Derivation of Equations (9) *and* (10)

First note that the Legendre polynomials $p_r(2t/T - 1)$, $t \in [0, T]$ satisfy (5), see Abramowitz and Stegun (1970). To simplify the notations, we replace without any loss in generality the interval $[0, T]$ by $[-T/2, T/2]$. The basis functions $f_r(t)$ are then related to the Legendre polynomials $p_r(x)$, $x \in [-1, 1]$, as $f_r(t) = p_r(\alpha t)$, with $t \in [-T/2, T/2]$ and $\alpha = 2/T$. Hence, the basis functions $f_r(t)$ satisfy the following recurrence formula

$$(r+1)\, f_{r+1}(t) = (2r+1)\, \alpha t f_r(t) - r f_{r-1}(t) \qquad (28)$$

for $r > 1$, with $f_0(t) = 1$ and $f_1(t) = \alpha t$, and where $f_{2r}(t)$ and $f_{2r+1}(t)$ are, respectively, even and odd functions of t (Abramowitz and Stegun, 1970).

We will prove the equivalence of the Laplace transforms of the outputs of the direct (7) and indirect (8) models. Since we shifted the time interval from $[0, T]$ to $[-T/2, T/2]$, the two-sided Laplace transform (Kwakernaak and Sivan, 1991) of the windowed signals is used, viz.

$$Y_0(s) = L\{y_0(t)\} = \int_{-T/2}^{+T/2} y_0(t)\, e^{-st} dt \qquad (29)$$

Applying the two-sided Laplace transform (29) to the indirect model (8) gives

$$Y_0(s) = \sum_{r=0}^{N_b} H_r(s)\, U_r(s) + T_H(s) \qquad (30)$$

with $U_r(s) = L\{u(t) f_r(t)\}$, and where $T_H(s)$ depends on the difference between the initial ($t = -T/2$) and final ($t = T/2$) conditions of the experiment (proof: follow the same lines of Pintelon and Schoukens, 1997). At the DFT frequencies $\omega_k = 2\pi k/N$, $T_H(j\omega)$ is a rational function of the frequency. A similar result is valid for the two-sided Laplace transform of the direct model (7)

$$Y_0(s) = \sum_{r=0}^{N_b} L\left\{f_r(t)\, L^{-1}\{G_r(s)\, U(s)\}\right\} + T_G(s) \qquad (31)$$

(proof: see Appendix A of Lataire *et al.*, 2012).

The proof consists in rewriting (30) under the form (31). In order to simplify the notations and calculations, the border effect terms $T_H(s)$ and $T_G(s)$ in (30) and (31) are discarded in the remainder of the proof. The equalities should be interpreted as being exact within a border effect term that is accounted for by $T_H(s)$ and $T_G(s)$. The key property used for calculating $U_r(s) = L\{u(t) f_r(t)\}$ in (30) is that $L\{t^p x(t)\} = (-1)^p X^{(p)}(s)$, where $X^{(p)}(s)$ is the p-th order derivative of $X(s)$ w.r.t s (Kwakernaak and Sivan, 1991). In the sequel of this appendix we elaborate explicitly the first three terms in the sum (30).

Since $f_0(t) = 1$, it follows immediately from (30) and (31) that $H_0(s)$ contributes to $G_0(s)$. Using $f(s) g^{(1)}(s) = (f(s) g(s))^{(1)} - f^{(1)}(s) g(s)$ the second term in (30) can be written as

$$\begin{aligned} H_1(s) U_1(s) &= \alpha H_1^{(1)}(s) U(s) - \alpha \left(H_1(s) U(s)\right)^{(1)} \\ &= \alpha H_1^{(1)}(s) U(s) + L\{f_1(t) z_1(t)\} \end{aligned} \qquad (32)$$

with $z_1(t) = L^{-1}\{H_1(s) U(s)\}$. Comparing (31) to (32) shows that $\alpha H_1^{(1)}(s)$ and $H_1(s)$ contribute to, respectively, $G_0(s)$ and $G_1(s)$. Proceeding in the same way, using $f(s) g^{(2)}(s) = (f(s) g(s))^{(2)} - 2(f^{(1)}(s) g(s))^{(1)} + f^{(2)}(s) g(s)$, we find an expression for the third term in (30)

$$\begin{aligned} H_2(s) U_2(s) = 1.5\alpha^2 H_2^{(2)}(s) U(s) + 3\alpha L\{f_1(t) w_2(t)\} + \\ L\{f_2(t) z_2(t)\} \end{aligned} \qquad (33)$$

with $w_2(t) = L^{-1}\{H_2^{(1)}(s) U(s)\}$ and $z_2(t) = L^{-1}\{H_2(s) U(s)\}$. Comparing (31) to (33) shows that $1.5\alpha^2 H_2^{(2)}(s)$, $H_2^{(1)}(s)$ and $H_2(s)$ contribute to, respectively, $G_0(s)$, $G_1(s)$ and $G_2(s)$.

Following the same lines for $N_b = 5$, we find (for notational simplicity we dropped the arguments)

$$\begin{aligned} G_0 = H_0 + \alpha \sum_{i=0}^{2} H_{2i+1}^{(1)} + \alpha^2 \left(\frac{3}{2} H_2^{(2)} + 5 H_4^{(2)}\right) + \\ \alpha^3 \left(\frac{5}{2} H_3^{(3)} + \frac{35}{2} H_5^{(3)}\right) + \alpha^4 \frac{35}{8} H_4^{(4)} + \alpha^5 \frac{63}{8} H_5^{(5)} \end{aligned} \qquad (34)$$

$$\begin{aligned} G_1 = H_1 + 3\alpha \sum_{i=1}^{2} H_{2i}^{(1)} + \alpha^2 \left(\frac{15}{2} H_3^{(2)} + 21 H_5^{(2)}\right) + \\ \alpha^3 \frac{35}{2} H_4^{(3)} + \alpha^4 \frac{315}{8} H_5^{(4)} \end{aligned} \qquad (35)$$

$$G_2 = H_2 + 5\alpha \sum_{i=1}^{2} H_{2i+1}^{(1)} + \alpha^2 \frac{35}{2} H_4^{(2)} + \alpha^3 \frac{105}{2} H_5^{(3)} \qquad (36)$$

$$G_3 = H_3 + 7\alpha H_4^{(1)} + \alpha^2 \frac{63}{2} H_5^{(2)} \tag{37}$$

$$G_4 = H_4 + 9\alpha H_5^{(1)} \tag{38}$$

$$G_5 = H_5 \tag{39}$$

which reveals the structure (9) and its bias term. Continuing the calculations till $N_b = 11$, gives the following α^0, α and α^2 contributions to G_r, $r = 0, 1, \ldots, 3$

$$G_0 = H_0 + \alpha \sum_{i=0}^{5} H_{2i+1}^{(1)} + \alpha^2 \Big(1.5G_2^{(2)} + 5G_4^{(2)} + \ldots \\ 10.5G_6^{(2)} + 18G_8^{(2)} + 27.5G_{10}^{(2)}\Big) \tag{40}$$

$$G_1 = H_1 + 3\alpha \sum_{i=1}^{5} H_{2i}^{(1)} + \alpha^2 \Big(7.5G_3^{(2)} + 21G_5^{(2)} + \ldots \\ 40.5G_7^{(2)} + 66G_9^{(2)} + 97.5G_{11}^{(2)}\Big) \tag{41}$$

$$G_2 = H_2 + 5\alpha \sum_{i=1}^{5} H_{2i+1}^{(1)} + \alpha^2 \Big(17.5G_4^{(2)} + 45G_6^{(2)} + \ldots \\ 82.5G_8^{(2)} + 130G_{10}^{(2)}\Big) \tag{42}$$

$$G_3 = H_3 + 7\alpha \sum_{i=2}^{5} H_{2i}^{(1)} + \alpha^2 \Big(31.5G_5^{(2)} + 77G_7^{(2)} + \ldots \\ 136.5G_9^{(2)} + 210G_{11}^{(2)}\Big) \tag{43}$$

and similarly for G_4, G_5, $\ldots$, G_{11}. It can be seen that the coefficients of the first order derivatives depend on the index $r = 0, 1, \ldots$ as $2r + 1$, which is consistent with (9). Differencing twice the coefficients of the second order derivatives in (40) gives the constant value two. Hence, the coefficients are a quadratic function of the coefficient index $i = 1, 2, \ldots$. Since the same is valid for the coefficients of the second order derivatives in (41)–(43), the corresponding coefficients in (40)–(43) can be written as

$$\beta_{2i,0} = 1.5 + 2.5(i-1) + (i-1)^2 \tag{44}$$
$$\beta_{2i,1} = 7.5 + 10.5(i-1) + 3(i-1)^2 \tag{45}$$
$$\beta_{2i,2} = 17.5 + 22.5(i-1) + 5(i-1)^2 \tag{46}$$
$$\beta_{2i,3} = 31.5 + 38.5(i-1) + 7(i-1)^2 \tag{47}$$

with $i = 1, 2, \ldots$. Differencing twice the coefficients of $(i-1)^0$, $(i-1)$ and $(i-1)^2$ in (44)–(47) gives the constant values four, four and zero, respectively. It shows that these coefficients are, respectively, quadratic and linear functions of the coefficient index $r = 0, 1, \ldots$, which motivates (10). Note that the special structure of Eqs. (34)–(47) is solely due to the particular recurrence formula (28), suggesting that it is valid for any value of N_b. To complete the proof an induction step is needed.

Induction Step

From the calculations in the previous section follows a general expression for the term $H_r(s)U_r(s)$ in the sum (30)

$$H_r U_r = L\left\{f_r(t) L^{-1}\{H_r U\}\right\} + \\ \alpha \sum_{i=0}^{\lfloor \frac{r-1}{2} \rfloor} \zeta_{r-2i-1} L\left\{f_{r-2i-1}(t) L^{-1}\left\{H_r^{(1)} U\right\}\right\} + \\ \alpha^2 \sum_{i=1}^{\lfloor \frac{r}{2} \rfloor} \beta_{2i,r-2i} L\left\{f_{r-2i}(t) L^{-1}\left\{H_r^{(2)} U\right\}\right\} + O\left(\alpha^3\right) \tag{48}$$

with $\zeta_n = 2n + 1$, $\beta_{2i,m}$ defined in (10), and where the arguments have been dropped for notational simplicity. Assuming that (48) is valid for $r, r-1, \ldots, 0$, we will show that it is valid for $r + 1$. Combining $H_{r+1}U_{r+1} = H_{r+1}L\{u(t)f_{r+1}(t)\}$ with (28) gives

$$\begin{aligned} H_{r+1}U_{r+1} &= -\alpha \frac{2r+1}{r+1} H_{r+1}U_r^{(1)} - \frac{r}{r+1} H_{r+1}U_{r-1} \\ &= -\alpha \frac{2r+1}{r+1} \left(H_{r+1}U_r\right)^{(1)} + \alpha \frac{2r+1}{r+1} H_{r+1}^{(1)} U_r \\ &\quad - \frac{r}{r+1} H_{r+1}U_{r-1} \end{aligned} \tag{49}$$

where the second equality uses $H_{r+1}U_r^{(1)} = (H_{r+1}U_r)^{(1)} - H_{r+1}^{(1)}U_r$. Applying (48) to $H_{r+1}U_r$, and calculating the derivative $(H_{r+1}U_r)^{(1)}$ using $X^{(1)}(s) = -L\{tL^{-1}\{X(s)\}\}$, one finds

$$-\alpha\left(H_{r+1}U_r\right)^{(1)} = L\left\{\alpha t f_r(t) L^{-1}\{H_{r+1}U\}\right\} + \\ \alpha \sum_{i=0}^{\lfloor \frac{r-1}{2} \rfloor} \zeta_{r-2i-1} L\left\{\alpha t f_{r-2i-1}(t) L^{-1}\left\{H_{r+1}^{(1)} U\right\}\right\} + \\ \alpha^2 \sum_{i=1}^{\lfloor \frac{r}{2} \rfloor} \beta_{2i,r-2i} L\left\{\alpha t f_{r-2i}(t) L^{-1}\left\{H_{r+1}^{(2)} U\right\}\right\} + O\left(\alpha^3\right) \tag{50}$$

Applying (48) to $\alpha H_{r+1}^{(1)}U_r$ and $H_{r+1}U_{r-1}$ gives, respectively,

$$\alpha H_{r+1}^{(1)} U_r = \alpha L\left\{f_r(t) L^{-1}\left\{H_{r+1}^{(1)} U\right\}\right\} + \\ \alpha^2 \sum_{i=0}^{\lfloor \frac{r-1}{2} \rfloor} \zeta_{r-2i-1} L\left\{f_{r-2i-1}(t) L^{-1}\left\{H_r^{(2)} U\right\}\right\} + O\left(\alpha^3\right) \tag{51}$$

$$H_{r+1}U_{r-1} = L\left\{f_{r-1}(t) L^{-1}\{H_{r+1}U\}\right\} + \\ \alpha \sum_{i=0}^{\lfloor \frac{r-2}{2} \rfloor} \zeta_{r-2i-2} L\left\{f_{r-2i-2}(t) L^{-1}\left\{H_{r+1}^{(1)} U\right\}\right\} + \\ \alpha^2 \sum_{i=1}^{\lfloor \frac{r-1}{2} \rfloor} \beta_{2i,r-2i-1} L\left\{f_{r-2i-1}(t) L^{-1}\left\{H_{r+1}^{(2)} U\right\}\right\} + O\left(\alpha^3\right) \tag{52}$$

Finally, collecting (49)–(52), taking into account that $\alpha t f_r(t) = \frac{r+1}{2r+1} f_{r+1}(t) + \frac{r}{2r+1} f_{r-1}(t)$ (see (28)), and similarly for $\alpha t f_{r-2i-1}(t)$ and $\alpha t f_{r-2i}(t)$, gives after some calculations (48) where r is replaced by $r+1$.

References

Abramowitz, M. and Stegun, I. A. (1970). *Handbook of Mathematical Functions*. New York: Dover Publications.

Abdel-Rahman, E. M., Nayfeh, A. H., and Masoud, Z. N. (2003). Dynamics and control of cranes: A review. *Journal of Vibration and Control*, vol. 9, no. 7, pp. 863-908.

Aguilera, R. P., Godoy, B. I., Agüero, J. C., Goodwin, G. C., and Yuz, J. I. (2014). An EM-based identification algorithm for a class of hybrid systems with application to power electronics. *International Journal of Control*, vol. 87, no. 7, pp. 1339-1351.

Allen, J. B. and Rabiner, L. R. (1977). A unified approach to short-time Fourier analysis and synthesis. *Proceedings of the IEEE,* vol. 65, no. 11, pp. 1558-1564.

Allen, M. S. (2008). Frequency-domain identification of linear time-periodic systems using LTI techniques. *Journal of Computational and Nonlinear Dynamics*, vol. 4, no. 4, article 041004, doi 10.1115/1.3187151.

Aerts, J. R. M. and Dirckx, J. J. J. (2010). Nonlinearity in eardrum vibration as a function of frequency and sound pressure. *Hearing Research*, vol. 263, no. 1-2, pp. 26-32.

Chen, S. Y., and Yuan, J. S. (2011). Adaptive gate bias for power amplifier temperature compensation. *IEEE Trans. on Device and Material Reliability*, vol. 11, no. 3, pp. 442-449.

Dimitriadis, G. and Cooper, J. E. (2001). Flutter prediction from flight flutter test data. *Journal of Aircraft*, vol. 38, no. 2, pp. 355-367.

Georgiev, A. A. (1989). On the identification of time-varying dynamic systems by nonparametric procedures. *IEEE Trans. on Autom. Contr.*, vol. 34, no. 2, pp. 223-225.

Hamilton, J. D. (1990). Analysis of time series subject to changes in regime. *Journal of Econometrics*, vol. 45, no. 1-2, pp. 39-70.

Kitagawa, G. and Gersch, W. (1985). A smoothness priors time-varying AR coefficient modeling of nonstationary covariance time series. *IEEE Trans. on Autom. Contr.*, vol. 30, no. 1, pp. 48-56.

Kwakernaak, H., and Sivan, R. (1991). *Modern Signals and Systems*. Englewood Cliffs: Prentice-Hall.

Lataire, J. and Pintelon, R. (2011). Frequency domain weighted nonlinear least squares estimation of continuous-time, time-varying systems. *IET Control Theory & Applications*, vol. 5, no. 7, pp. 923-933.

Lataire, J., Pintelon, R. and Louarroudi, E. (2012). Non-parametric estimate of the system function of a time-varying system. *Automatica*, vol. 48, no. 4, pp. 666-672.

Li, Y. and Billings, S. A. (2011). Identification of time-varying systems using multi-wavelet basis functions. *IEEE Trans. on Contr. Systems*, vol. 19, no. 3, pp. 656-663.

Liu, K. (1997). Identification of linear time-varying systems. *Journal of Sound and Vibration*, vol. 206, no. 4, pp. 487-505.

Louarroudi, E., Lataire, J., Pintelon, R., Janssens P., and Swevers, J. (2013). Frequency domain, parametric estimation of the evolution of the time-varying dynamics of periodically time-varying systems from noisy input-output observations. Mechanical Systems and Signal Processing, doi 10.1016/j.ymssp.2013.03.013.

Louarroudi, E., Pintelon, R. and Lataire, J. (2012). Nonparametric tracking of the time-varying dynamics of weakly nonlinear periodically time-varying systems using periodic inputs. *IEEE Trans. on Instrum. and Meas.*, vol. 61, no. 5, pp. 1384-1394.

Niedzwiecki, M. (2000). *Identification of Time-Varying Processes*. Chichester: J. Wiley & Sons.

Niedzwiecki, M. and Kaczmarek, P. (2005). Identification of quasi-periodically varying systems using the combined nonparametric/parametric approach. *IEEE Trans. on Sign. Proc.*, vol. 53, no. 12, pp. 4588-4598.

Paoletti, S., Juloski, A. Lj., Ferrari-Trecate, G., and Vidal, R. (2007). Identification of hybrid systems – A tutorial. *European Journal of Control*, vol. 13, no. 2-3, pp. 242-260.

Pintelon, R., Louarroudi, E. and Lataire, J. (2012). Detection and quantification of the influence of time-variation in frequency response function measurements using arbitrary excitations. *IEEE Trans. Instrum. and Meas.*, vol. 61, no. 12, pp. 3387-3395.

Pintelon, R. and Schoukens, J. (1997). Identification of Continuous-Time Systems Using Arbitrary Signals. *Automatica*, vol. 33, no. 5, pp. 991-994.

Pintelon, R., and Schoukens, J. (2012). *System Identification: A Frequency Domain Approach*. 2nd edition, Hoboken (USA): Wiley – IEEE Press.

Pintelon, R., Schoukens, J., Vandersteen, G., and Barbé, K. (2010). Estimation of nonparametric noise and FRF models for multivariable systems - Part I: theory. *Mechanical Systems and Signal Processing*, vol. 24, no. 3, pp. 573-595.

Pop, V., Bergveld, H. J., Notten, P. H. L., and Regtien, P. P. L. (2005). State-of-the-art of battery state-of-charge determination. *Measurement Science & Technology*, vol. 16, no. 12, pp. R93-R110.

Poulimenos, A. G. and Fassois, S. D. (2006). Parametric time-domain methods for non-stationary random vibration modelling and analysis - A critical survey and comparison. *Mechanical Systems and Signal Processing*, vol. 20, no. 4, pp. 763-816.

Ralston, A. and Rabinowitz, P. (1984). *A First Course in Numerical Analysis*. New York (USA): McGraw-Hill.

Rodrigues, S., Munichandraiah, N., and Shukia, A. K. (2000). A review of state-of-charge indication of batteries by means of a.c. impedance measurements. *Journal of Power Sources*, vol. 87, no. 1-2, pp.12-20.

Sanchez, B., Louarroudi, E., Bragos, R., and Pintelon R. (2013). Harmonic impedance spectra identification from time-varying bioimpedance: theory and validation. Physiological Measurement, vol. 34, no. 10, pp. 1217-1238 (doi 10.1088/0967-3334/34/10/1217).

Sams, A. D. and Marmarelis, V. Z. (1988). Identification of linear periodically time-varying systems using white-noise test inputs. *Automatica*, vol. 24, no. 4, pp. 563-567.

Schoukens, J., Vandersteen, G., Barbé, K., and Pintelon, R. (2009). Nonparametric preprocessing in system identification: a powerful tool. *European Journal of Control*, vol. 15, no. 3-4, pp. 260-274.

Spiridonakos, M. D. and Fassois, S. D. (2009). Parametric identification of a time-varying structure based on vector vibration response measurements. *Mechanical Systems and Signal Processing*, vol. 23, no. 6, pp. 2029-2048.

Tóth, R., Laurain, V., Gilson, M., and Garnier, H. (2012). Instrumental variable scheme for closed-loop LPV model identification. *Automatica*, vol. 48, no. 9, pp. 2314-2320.

Tsatsanis, M. K. and Giannakis, G. B. (1993). Time-varying system-identification and model validation using wavelets. *IEEE Trans. on Sign. Proc.*, vol. 41, no. 12, pp. 3512-3523.

Van Ingelgem, Y., Tourwé, E., Vereecken, J. and Hubin, A. (2008). Application of multisine impedance spectroscopy, FE-AES and FE-SEM to study the early stages of copper corrosion. *Electrochemica Acta*, vol. 53, no. 25, pp. 7523-7530.

Yin, G. G., Kan, S., Wang, L. Y., and Xu, C. Z. (2009). Identification of systems with regime switching and unmodeled dynamics. *IEEE Trans. Autom. Contr.*, vol. 54, no. 1, pp. 34-47.

Zadeh, L. A. (1950a). The determination of the impulsive response of variable networks. *Journal of Applied Physics*, vol. 21, pp. 642-645.

Zadeh, L. A. (1950b). Frequency analysis of variable networks. *Proceedings of the I.R.E.*, vol. 38, pp. 291-299.